Rapid fabrication of micro-nanometric tapered fiber lens and characterization by a novel scanning optical microscope with submicron resolution

Shouguo Zheng,[1,3] Xinhua Zeng,[1,*] Wei Luo,[1] Safi Jradi,[2] Jérôme Plain,[2] Miao Li,[1] Philippe Renaud-Goud,[2] Régis Deturche,[2] Zengfu Wang,[1] Jieting Kou,[1] Renaud Bachelot[2] and Pascal Royer[2]

[1]*Institute of Intelligent machines, Chinese Academy of Sciences, 350, Road Shushan Lake, 230031 Hefei, China*
[2]*Laboratoire de Nanotechnologie et d'Instrumentation Optique, Université de technologie de Troyes, 12, rue Marie Curie - BP 2060, 10010 Troyes, France*
[3]*Anhui Institute of Optics and Fine Mechanics, Chinese Academy of Sciences, Hefei 230031, China*
[*]*xhzeng@iim.ac.cn*

Abstract: In numerous applications of optical scanning microscopy, a reference tapered fiber lens with high symmetry at sub-wavelength scale remains a challenge. Here, we demonstrate the ability to manufacture it with a wide range of geometry control, either for the length from several hundred nanometers to several hundred microns, or for the curvature radius from several tens of nanometers to several microns on the endface of a single mode fiber. On this basis, a scanning optical microscope has been developed, which allows for fast characterization of various sub-wavelength tapered fiber lenses. Focal position and depth of microlenses with different geometries have been determined to be ranged from several hundreds of nanometers to several microns. FDTD calculations are consistent with experimental results.

OCIS codes: (060.2340) Fiber optics components; (110.2350) Fiber optics imaging; (180.5810) Scanning microscopy; (080.3630) Lenses.

References and links

1. M. He, X. C. Yuan, N. Q. Ngo, J. Bu, and S. H. Tao, "Low-cost and efficient coupling technique using reflowed sol-gel microlens," Opt. Express **11**(14), 1621–1627 (2003).
2. S. M. Yeh, S. Y. Huang, and W. H. Cheng, "A new scheme of conical-wedge-shaped fiber endface for coupling between high-power laser diodes and single-mode fibers," J. Lightwave Technol. **23**(4), 1781–1786 (2005).
3. Y. K. Lu, Y. C. Tsai, Y. D. Liu, S. M. Yeh, C. C. Lin, and W. H. Cheng, "Asymmetric elliptic-cone-shaped microlens for efficient coupling to high-power laser diodes," Opt. Express **15**(4), 1434–1442 (2007).
4. F. X. Gu, H. K. Yu, P. Wang, Z. Y. Yang, and L. M. Tong, "Light-emitting polymer single nanofibers via waveguiding excitation," ACS Nano **4**(9), 5332–5338 (2010).
5. X. Michalet, F. F. Pinaud, L. A. Bentolila, J. M. Tsay, S. Doose, J. J. Li, G. Sundaresan, A. M. Wu, S. S. Gambhir, and S. Weiss, "Quantum dots for live cells, in vivo imaging, and diagnostics," Science **307**(5709), 538–544 (2005).
6. D. J. Stephens and V. J. Allan, "Light microscopy techniques for live cell imaging," Science **300**(5616), 82–86 (2003).
7. J. G. White and W. B. Amos, "Confocal microscopy comes of age," Nature **328**(6126), 183–184 (1987).
8. D. L. Stokes and T. Vo-Dinh, "Development of an integrated single-fiber SERS sensor," Sens. Actuators B Chem. **69**(1-2), 28–36 (2000).
9. C. Viets and W. Hill, "Comparison of fibre-optic SERS sensorswith differently prepared tips," Sens. Actuators B Chem. **51**(1-3), 92–99 (1998).
10. E. J. Smythe, M. D. Dickey, J. Bao, G. M. Whitesides, and F. Capasso, "Optical antenna arrays on a fiber facet for in situ surface-enhanced Raman scattering detection," Nano Lett. **9**(3), 1132–1138 (2009).
11. F. L. Yap, P. Thoniyot, S. Krishnan, and S. Krishnamoorthy, "Nanoparticle cluster arrays for high-performance SERS through directed self-assembly on flat substrates and on optical fibers," ACS Nano **6**(3), 2056–2070 (2012).

#175636 - $15.00 USD Received 5 Sep 2012; revised 1 Nov 2012; accepted 7 Dec 2012; published 2 Jan 2013

12. L. W. Lo, P. J. Tsai, S. H. Y. Huang, W. Y. Chen, Y. T. Wang, C. H. Chang, and C. S. Yang, "In vivo monitoring of fluorescent nanosphere delivery in anesthetized rats using an implantable fiber-optic microprobe," Anal. Chem. **77**(4), 1125–1131 (2005).
13. X. H. Zeng, J. Plain, S. Jradi, P. Renaud-Goud, R. Deturche, P. Royer, and R. Bachelot, "High speed sub-micrometric microscopy using optical polymer microlens," Chin. Opt. Lett. **7**, 901–903 (2009).
14. T. Ichimura, N. Hayazawa, M. Hashimoto, Y. Inouye, and S. Kawata, "Tip-enhanced coherent anti-stokes Raman scattering for vibrational nanoimaging," Phys. Rev. Lett. **92**(22), 220801 (2004).
15. R. P. Barretto, B. Messerschmidt, and M. J. Schnitzer, "In vivo fluorescence imaging with high-resolution microlenses," Nat. Methods **6**(7), 511–512 (2009).
16. H. Ibn El Ahrach, R. Bachelot, A. Vial, G. Lérondel, J. Plain, P. Royer, and O. Soppera, "Spectral degeneracy breaking of the plasmon resonance of single metal nanoparticles by nanoscale near-field photopolymerization," Phys. Rev. Lett. **98**(10), 107402 (2007).
17. C. Deeb, R. Bachelot, J. Plain, A. L. Baudrion, S. Jradi, A. Bouhelier, O. Soppera, P. K. Jain, L. Huang, C. Ecoffet, L. Balan, and P. Royer, "Quantitative analysis of localized surface plasmons based on molecular probing," ACS Nano **4**(8), 4579–4586 (2010).
18. C. Deeb, C. Ecoffet, R. Bachelot, J. Plain, A. Bouhelier, and O. Soppera, "Plasmon-based free-radical photopolymerization: effect of diffusion on nanolithography processes," J. Am. Chem. Soc. **133**(27), 10535–10542 (2011).
19. H. L. Ren, C. Jiang, W. S. Hua, M. Y. Gao, J. Y. Wang, H. Wang, J. T. He, and E. J. Liang, "The preparation of optical fibre nanoprobe and its application in spectral detection," Opt. Laser Technol. **39**(5), 1025–1029 (2007).
20. N. Axelrod, A. Lewis, N. B. Yosef, R. Dekhter, G. Fish, and A. Krol, "Small-focus integral fiber lenses: modeling with the segmented beam-propagation method and near-field characterization," Appl. Opt. **44**(7), 1270–1282 (2005).
21. E. B. Li, "Characterization of a fiber lens," Opt. Lett. **31**(2), 169–171 (2006).
22. H. E. Williams, D. J. Freppon, S. M. Kuebler, R. C. Rumpf, and M. A. Melino, "Fabrication of three-dimensional micro-photonic structures on the tip of optical fibers using SU-8," Opt. Express **19**(23), 22910–22922 (2011).
23. M. Malinauskas, A. Zukauskas, V. Purlys, K. Belazaras, A. Momot, D. Paipulas, R. Gadonas, A. Piskarskas, H. Gilbergs, A. Gaidukeviciute, I. Sakellari, M. Farsari, and S. Juodkazis, "Femtosecond laser polymerization of hybrid/integrated micro-optical elements and their characterization," J. Opt. **12**(12), 124010 (2010).
24. M. Hocine, N. Fressengeas, G. Kugel, C. Carre, D. J. Lougnot, R. Bachelot, and P. Royer, "Modeling the growth of a polymer microtip on an optical fiber end," J. Opt. Soc. Am. B **23**(4), 611–620 (2006).
25. X. H. Zeng, J. Plain, S. Jradi, C. Darraud, F. Louradour, R. Bachelot, and P. Royer, "Integration of polymer microlens array at fiber bundle extremity by photopolymerization," Opt. Express **19**(6), 4805–4814 (2011).
26. C. Y. Chang, S. Y. Yang, L. S. Huang, and T. M. Jeng, "A novel method for rapid fabrication of microlens arrays using micro-transfer molding with soft mold," J. Micromech. Microeng. **16**(5), 999–1005 (2006).
27. G. Lérondel, S. Kostcheev, and J. Plain, "Nanofabrication for plasmonics," Springer Se. Opt. Sci. **167**, 269–316 (2012).

1. Introduction

The coupling efficiency between a laser diode and a single-mode fiber is an issue of great importance and has been pursued by researchers aiming to promote the applications of active or passive optical fiber devices [1–3]. Due to very small core size of the single-mode fiber (several microns) and relatively low numerical aperture (NA, at the order of 0.1), high coupling efficiency between them encounters great challenges. The introduction of a tapered microlens either on the endface of an optical fiber or on the surface of the counterpart optical components is essential to improve the numerical aperture value of the fiber coupling system, therefore significantly increases the coupling efficiency. It enables the study of light-emitting for even a single nanofibers via waveguiding excitation [4]. Imaging optically a single cell or living cell is of interests in biology [5,6]. While the labeling agents and skills are burgeoning, the exploration of optical imaging instruments remains undeveloped since the significant advance of confocal microscope by White and Amos [7]. The expensive cost of the high precision optical system is a major drawback. Optical fiber is demonstrated to be a alternative tool for an insight study on cell molecules or samples in vivo. Surface-enhanced Raman scattering (SERS) based on single optical fiber facet permit their corresponding studies in situ [8–11]. Using an implantable optical fiber taper, fluorescent nanosphere delivery in anesthetized rats can be monitored in vivo [12]. Nevertheless, the time-consuming fabrication process by chemical etching and the difficulty for geometrical perfection of fiber taper limit its applications. Recently, a scanning optical microscope (SOM) based on a tapered fiber

#175636 - $15.00 USD Received 5 Sep 2012; revised 1 Nov 2012; accepted 7 Dec 2012; published 2 Jan 2013

microlens fabricated by a fast photo-polymerization technique was reported [13]. A sub-micrometric resolution has been achieved by this novel technique, which is better than the confocal microscope. It is potential for the Raman-tagged or fluorescent-marked single cell imaging [14,15], and essential to study local effects such as the area-selective polarization or local enhancement in nanophotonics [16–18].

The investigation and understanding in-depth for the optical properties of fiber lens is essential for either coupling or imaging applications. These optical characteristics of the tapered fiber lens depend on their geometry, including the curvature radius and length. Generally, the geometry of the tapered fiber microlens is conical or cylindrical with high symmetry. Nevertheless, various different geometries have been reported: quadrangular-pyramid-shaped fiber endface (QPSFE), hemi-spherical microlens (HSM), double-variable-curvature fiber endface (DVCFE), and asymmetric hyperbolic fiber microlens (AHFM) [3]. The asymmetry may cause a dramatic decrease of coupling efficiency and may be disastrous for SOM. So far, three major technologies have been developed for the realization of the tapered fiber microlens, namely mechanical pulling while being heated by electric arc or laser [19], chemical etching by hydrofluoride (HF) [19] and photo-polymerization [13]. The advantage of the first technique is that the fabrication process is rapid, whereas its disadvantages include the high transmission loss since the core is reduced to several tens of nanometers, and the ease of asymmetry formation. The second method has partially resolved the transmission loss, whereas it is a time-consuming process. The third involves a photo-tunable process in several minutes, which provides a reproducible geometry with high symmetry in spite of a reduced mechanical robustness due to the polymer-fiber junction.

The manufacture of tapered fiber lens of several tens of or several hundreds of microns of curvature radius have been reported [20–23]. Theoretical calculation was performed on their focal position and focal length [20, 21]. Additionally, the experimental measurement is based on 2D or 3D profile record by a digital CCD [20, 21, 23] or on reflection method [22]. Up to date, the characterization of tapered structures concerning their focal position and focal depth is still a challenge to some extent, since they ranged from several tens of nanometers to a few tens of microns.

In this letter, we will demonstrate a novel approach using a newly self-designed and manufactured SOM with high scanning speed to characterize the fiber microlens. We will firstly present a simple and convenient route to fabricate polymer tapered microlens with symmetric end shape and tunable curvature radius at the endface of an optical fiber. On the basis of the successful fabrication work, we will then describe the development of a high speed SOM that can realize the imaging of a nano-scaled metal sample. We will demonstrate the capability to characterize rapidly the focal position and focal depth of different polymer tapered microlens by using this SOM system. Finally, a finite difference time domain (FDTD) calculation will be performed to support our experimental results.

2. Experimental

The principle of free-radical photo-polymerization method is presented in detail in Ref [24, 25]. The photosensitive solution consists of three components: a photosensitive dye, an amine cosynergist and a multifunctional acrylate monomer. Herein, two types of photosensitive dyes were used. One is Eosin Y, which is highly sensitive in the spectral range from 450 to 550 nm (the maximum absorption of Eosin Y dye is centered at 517 nm). Its absorbance and molecular formula are listed in Fig. 1(a). Therefore, a frequency-doubled Nd/YAG laser (532 nm) is suitable for the fabrication of fiber tapered microlens while using Eosin Y. As shown in Fig. 1(b), a droplet of the above-mentioned formulation is placed on the endface of a well cleaved single mode optical fiber with a core radius of 1.3 μm. A laser beam with tunable intensity coupled to the fiber allows to induce the photo-polymerization. Owing to the Gaussian form of the laser beam, a tiny polymer lens is formed. Due to a small difference of refractive index between the polymer (n = 1.52) and the unpolymerized formulation (n =

#175636 - $15.00 USD Received 5 Sep 2012; revised 1 Nov 2012; accepted 7 Dec 2012; published 2 Jan 2013

1.48), the polymer then acts as a guide who makes the tiny lens confine the laser beam and permits the oriented polymerization along the axis direction. Finally, the polymer tapered lens appears after removing the unpolymerized formulation by a rinsing step in ethanol. In this case, the curvature radius of a fiber lens is limited down to several hundred nanometers. In order to obtain smaller ones, Irgacure 819 is used instead of Eosin Y as photosensitive dye. It is highly sensitive under 400 nm but still absorbs in the visible, as shown in Fig. 1(a). A polymer tapered lens is first shaped with an energy just higher than its threshold by 532 nm laser. Then it is reinforced using a 405 nm laser after the unpolymerized formulation around it being developed. By this method, the fiber tapered lens can be obtained with a radius of curvature down to several tens nanometers.

On the basis of polymer tapered microlens manufacture, a high speed scanning optical microscope has been developed recently in our laboratory. As shown in Fig. 1(c), a single mode fiber with a polymer tip at the extremity was used here as a local light source to illuminate the sample. The optical signal can be then collected by a photodetector either in reflection or transmission mode. The sample was placed on an auto-controlling XY stage with a maximal scanning speed of 250 mm/s and a minimal scanning step of 50 nm. The approaching process was precisely controlled using a home-made routine, which allows a minimal step (along Z axis) of 30 nm. The sample illumination and the reflected signal detection is realized by the same Y-coupler, whereas the transmitted signal is directly detected by a photomultiplier (PMT) being installed below the illuminating fiber lens.

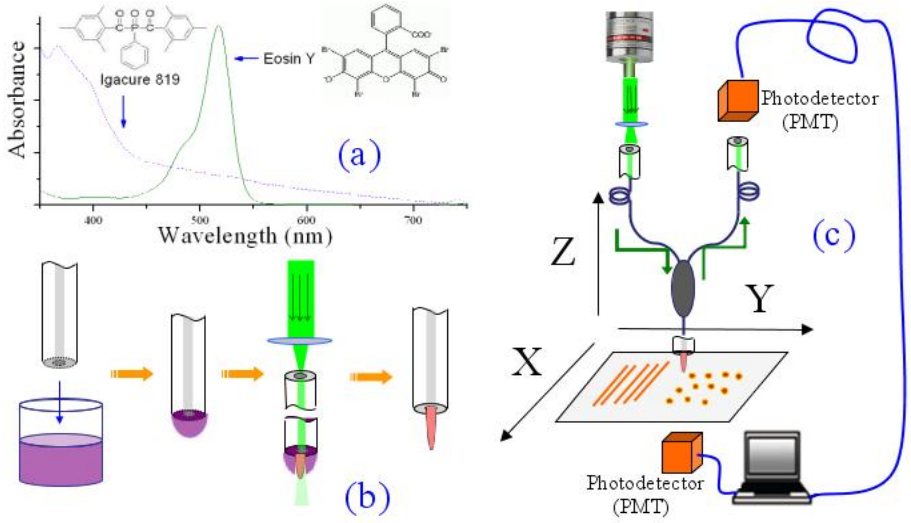

Fig. 1. Scanning optical microscope based on tapered fiber lens. (a) Molecular formula and absorbance spectra of Eosin Y and Irgacure 819, respectively. (b) Schematic of polymer tapered microlens manufacture on the distal face of an optical fiber. A cleaved optical fiber is dipped into the photosensitive solution and then photo-polymerized by a laser beam. After being washed in ethanol, the fiber lens formed at the optical fiber end. (c) Schematic of the experimental setup of a high speed scanning optical microscope using a tapered fiber polymer microlens. The sample is scanned along XY plane with a minimal step of 50 nm, whereas the fiber microlens is fixed right above the photodetector in transmission. The incident laser beam and the signal by reflection is realized by a Y-shaped coupler. The motion along Z-axis is controlled by a motor with a minimal step of 30 nm and feedbacked by the interfere between the reflective and incident laser beam.

#175636 - $15.00 USD Received 5 Sep 2012; revised 1 Nov 2012; accepted 7 Dec 2012; published 2 Jan 2013

3. Analysis and discussions

3.1 Optimizing curvature radius via addition of inhibitors

The curvature radius of the tapered lens is of great importance for the scanning optical microscopy. For a scanning optical microscope, particularly in scanning near field optical microscope, there will be a lateral enlargement of the sample, in particular in the case where the curvature radius is much bigger than the nanoparticle. This difference will give rise to a fatal deviation of the experimental results. Therefore, smaller radius is expected for these applications. It can be realized by the inhibition of the lateral growth, either by reducing free radicals during the polymerization or shortening the time of exited state. We hereby prefer to use the first strategy that may be realized by introducing other free radicals to compete or result in the end of the chain reaction, which leads to the increase of the threshold for the polymerization. Figure 2 shows tapered fiber lenses on the endface of a single-mode fiber (with a core radius of 1.3 μm) obtained through the photo-polymerization of undoped formulation or doped by 4-Methoxyphenol of 1-30% in weight as an inhibitor. Considering the photonic conditions, illumination through a single-mode optical fiber with Gaussian intensity profile, only a reduced area of the core can satisfy the polymerization condition by overpassing the threshold. Using this strategy, tapered fiber lens with several tens nanometers can be obtained (Fig. 2(d)), which is potential for scanning near-field optical microscopy (SNOM).

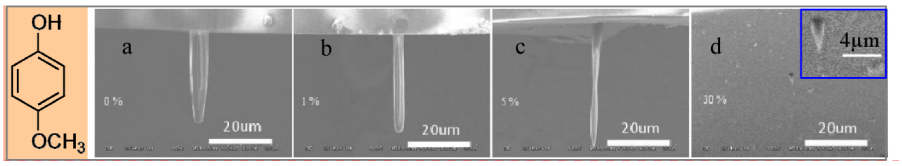

Fig. 2. Tapered fiber lens fabricated by addition of inhibitor. The addition of 4-Methoxyphenol (left) results in an increase of the polymerization threshold, hence confines the lateral growth from the initial stage. With a large amount (up to 30% in weight) of 4-Methoxyphenol addition, the polymerization along axis direction can also be suppressed. (a) without inhibitor, (b) with 1% inhibitor, (c) with 5% inhibitor, d) with 30% inhibitor. The tiny fiber lens is specified by a red-doted circle. For all these results, the same exposure dose of E = 10 μJ (5 μW and 2 s) is applied.

3.2 Nanometric lens integrated directly on microlens

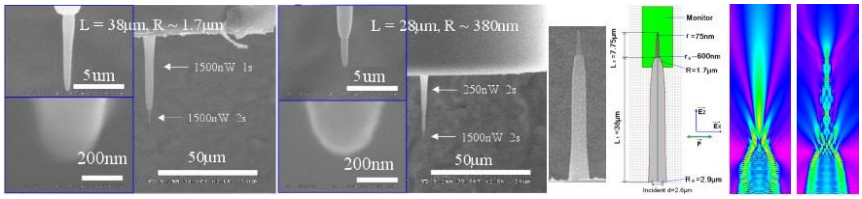

Fig. 3. Nanometric lens integrated directly on microlens. Two steps are concerned for the fabrication of this complex structure. The first step is the manufacture of a big micrometric lens on the fiber endface with a formulation without inhibitor addition. The second step is the further integration of a smaller lens with radius of some tens nanometers in just few seconds. (a) 1500 nW for 1s and 1500 nW for 2 s for the first step and second step, respectively. (b) 250 nW for 2 s and 1500 nW for 2 s for the two steps, respectively. L1 = 28μm, R1 = 380nm; L2 = 3.25μm, R2 = 120nm. (c) 2D FDTD calculation of the complex tapered structure. The structure is taken from a) with L1 = 38 μm, R1 = 1.7 μm, L2 = 7.75 μm and R2 = 75 nm. The diameter for the two lenses at the bottom is 5.8 μm and 1.2 μm, respectively. On the right, electric field component of /Ex/ for the case without (left) and with (right) a nanometric lens on the microlens are displayed, respectively. Actually,the curvature radius of microlens and nanometric lens are obtained by measurement and fitting from the enlarged SEM image.

#175636 - $15.00 USD Received 5 Sep 2012; revised 1 Nov 2012; accepted 7 Dec 2012; published 2 Jan 2013

In certain case of applications, an oblique angle is indispensable. Consequently, the length of the tapered fiber lens should at least be several tens of microns. For the application such as SNOM, the smallest radius is desired. To reach both standards, a nanometric lens has been integrated directly on the extremity of a tapered fiber microlens. As shown in Fig. 3, a microlens with a curvature radius of several microns (Fig. 3(a)) or several hundred nanometers (Fig. 3(b)) is first fabricated directly on the endface of a single-mode fiber. In both cases, a formulation without inhibitor addition is used. For the first one (Fig. 3(a)), an irradiation power is 1500 nW for 1 s, which gives rise to a tapered polymer lens with a curvature radius of 1.7 μm and a length of 38 μm. For the second one (Fig. 3(b)), an irradiation dose of 250 nW for 2 s is used. It leads to the formation of a tapered lens with a 380 nm curvature radius and a 28 μm in length. Subsequently, using the formulation with 7.5% 4-Methoxyphenol (optimized concentration determined by a careful systematic study), a smaller tapered lens is integrated exactly on the extremity of the micrometric polymer lens. The photo-polymerization condition for both cases is the same as 1500 nW for 2 s. Some tens of nanometric curvature radius can be achieved for this second step. In order to describe the guiding property of this complex tapered structure, a FDTD simulation of two dimensions (2D) is performed based on its geometry. Figure 3(c) displays the parameters' design for the simulation on the left. The incident light width is assumed to 2.6 μm, which is the same as the mode field diameter of the single-mode fiber used here. The monitor (in green color) is placed to the end of the first lens and encasing the second one. On its right, the results of electric field component of $/E_x/$ without and with the nanometric tapered lens are displayed, respectively. A more confined spot size can be achieved after the guiding of the second nanometric lens.

3.3 Development of SOM and its use for fiber optics polymer lens characterization

Usually, beam profile is used for the characterization of the optical properties of microlens with a focal position of several tens or several hundred microns [26]. It encounters difficulty to characterize a fiber lens with a focal position at micro-nanometric scale. In order to overpass this limitation, we developed a novel scanning microscope based on the tapered fiber lens. Figure 4 (a) shows a gold Asian umbrella nanostructured sample fabricated by electron-beam lithography method [27]. It plays a role as a standard sample in the following experiments. The width and the period of the skeleton at the edge are 500 nm and 1 μm, respectively. Both these two values decrease from the first layer at the edge to the sixth layer at the center, and becomes 50 nm and 100 nm, respectively. The tapered fiber microlens used here is fabricated by using an irradiation power of 500 nW for 2 s on the distal of a single-mode fiber. Its length is about 30 μm, and the curvature radius at the end is about 1725 nm. The diameter at the bottom from the distal face of the optical fiber is about 5.5 μm. It should be noted that this value is much bigger than the core diameter (2.6 μm) of the single-mode fiber. Optical images were obtained using a constant working distance mode. Both optical signals in transmission and reflection were collected for each constant position. Figure 4(b) shows the optical image of the umbrella sample at a distance of 2100 nm using the data collected by the photodetector in transmission. An increase of resolution has been found at the initial stage while the fiber microlens approaching the sample. After a critic distance, the images have been found to get worse. Figures 4 (c) and 4(d) present two optical images for the umbrella sample with different distances between the sample and the microlens tip, 300 nm and 2100 nm, respectively. It is intuitive that the image obtained for a distance of 2100 nm is better (in term of contrast) than the other one (obtained at 300nm). In other words, it means that 2100 nm is closer to the focal point than 300 nm. For a complete characterization, a systematic study of the contrast evolution with the distance (from contact to 6000 nm) has been performed. A circle profile (red dotted line in Fig. 4(d)) at the same axial position is selected for all sequences' analysis. In order to simplify the comparison, a Fourier fit was used to treat all these periodic profiles. Selected results of the original data and their corresponding

#175636 - $15.00 USD Received 5 Sep 2012; revised 1 Nov 2012; accepted 7 Dec 2012; published 2 Jan 2013

fitted results have been presented in Fig. 4(f). Due to different reflection or transmission efficiency between the gold umbrella and the glass substrate, an optical contrast either for reflection or transmission has been defined. Thus, we define $C = 2(\overline{Y_{bright}} - \overline{Y_{dark}}) / (\overline{Y_{bright}} + \overline{Y_{dark}})$ as a criterion for the relative contrast. In which, $\overline{Y_{bright}}$ is the averaged valueof the maximal intensity, $\overline{Y_{dark}}$ is the averaged value of the minimal intensity. By using this criterion, we plot the contrast as a function of the distance, as shown in Fig. 4(e). The maximum of the contrast value is obtained for a distance of about 2 μm. A contrast value up to 1.3 ± 0.1 is found in the range from 1 μm to about 2.5 μm. On one hand, in the reflection mode, the experimentally determined focal position is 2μm and the focal depth is about 1.5μm, respectively. In a similar way in the transmitted mode, we found that the focal position and the focal depth for this polymer microlens corresponds to 2.3 μm and 2 μm, respectively. Note that for a distance of about 2 μm, a high resolution of about 150nm can be achieved.

We have also studied two other polymer microlens, among which one is bigger and the other is smaller than this first microlens. We found the focal position of 5 μm and focal depth of 3-5 μm both in transmission and reflection measurement for the microlens with a radius of 5900 nm, which is fabricated using 1500 nW to irradiate for 2 s. A focal position of 0.5 μm and focal depth of 0.5 μm via reflection measurement for a microlens with a radius of 440 nm being fabricated by 250 nW for 1 s. These experimentally measured results are listed in Table 1.

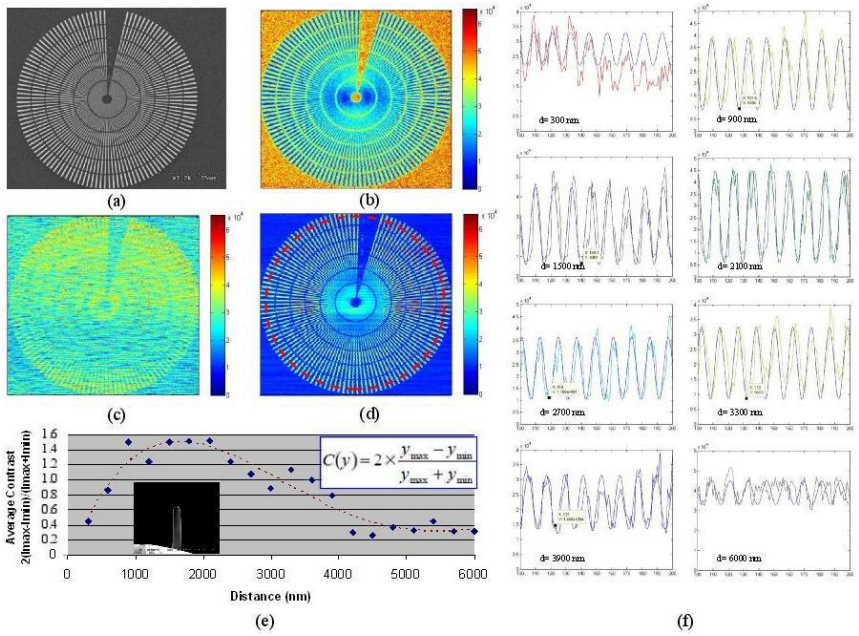

Fig. 4. Optical characterization of microlens. (a) Nanometric periodic gold Asian umbrella by electron -beam lithography serves as a standard sample. The width of the skeleton diminishes from 500 nm at the edge to 50 nm at the center. (b) showing optical image by transmission of the gold sample obtained at a distance of 2100 nm. (c) and (d) showing optical images by reflection for distances of 300 nm and 2100 nm, respectively. (e) Relative contrast values on the distances between sample and fiber microlens. (f) Selected profiles by reflection for different distances. The X coordinate axe corresponds to the scanning step number. The Y coordinate axe corresponds to the intensity for each scanning step.Different color is presented for the measured data with different distance. And the dark-gray line represents the fitting curves for all cases. For all measurements, the same fiber microlens with a curvature radius of 1725 nm and length of 30 microns is used, which is realized using 500 nW green laser beam (532 nm) to irradiate for 2 s.

#175636 - $15.00 USD Received 5 Sep 2012; revised 1 Nov 2012; accepted 7 Dec 2012; published 2 Jan 2013

In order to further confirm the experimental results by SOM measurement, FDTD calculations were performed for these polymer probes. A small grid size of 10 nm is used for the simulation. The simulation may be conducted in three-dimensions (3D). However, as the polymer microlens is axially perfectly symmetric, we performed the calculations in 2-dimensions. In this simulation, electric field ($/E_x/$, $/E_z/$) and Poynting vector were chosen as the spatial outputs. The former can record the electric field components ($/E_x/$, $/E_z/$) over the monitor domain at specific points in time, whereas the Poynting vector can be regarded as representing the energy flux (in W/m^2) of an electromagnetic field. Similar results can be obtained for these three components. We hereby present only the electric field components $/E_x/$ in Fig. 5 for each fiber lens calculation. The structure design for the simulation is a perfect copy of the shape determined from SEM images of the microlens. In the first case, the diameter at the junction part is 7.6 μm, and the radius at the end is 5900 nm. Its length is estimated to be 30.4 μm. FDTD calculation shows that the focal position in this case is 5 μm with a large focal depth up to about 4 μm. In the second case with the diameter at the junction part of 5.5 μm, the radius of 1725 nm at the end and the length of 30 μm, the focal position is calculated to be 1.8 μm and the focal depth is up to about 2 μm. In the last case for a small microlens with a diameter at the junction part of 4.4 μm, the curvature radius of 440 nm at the end and the length of 33.5 μm, the focal position is calculated as short as 0.25 μm from its tip end. The focal depth can be regarded as about 0.5 μm. These typical results are in good agreements with measured focal position and focal depth either in transmission or in reflection. For comparison, all calculated results are also listed in Tab. 1.

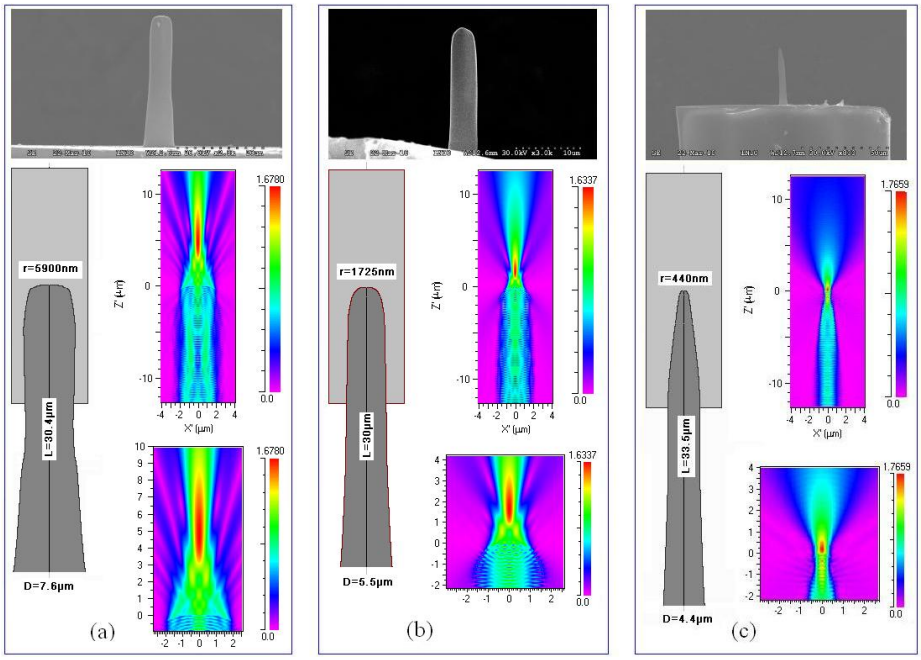

Fig. 5. FDTD calculation for microlens. Up: SEM images of three tapered fiber microlens with different geometry. Down: The structure design for FDTD calculation and corresponding results with two different magnifications. (a) 1500 nW and 2 s; (b) 500 nW and 2 s,; (c) 250 nW and 1 s.

#175636 - $15.00 USD Received 5 Sep 2012; revised 1 Nov 2012; accepted 7 Dec 2012; published 2 Jan 2013

Table 1. Focal position and focal depth of fiber microlens. Experimental results both by reflection and transmission measurements of focal position and focal depth for three microlens with different geometry. The corresponding FDTD calculation results are also listed.

Radius (nm)	Length (μm)	Focal position by transmission (μm)	Focal depth by transmission (μm)	Focal position by reflection (μm)	Focal depth by reflection (μm)	Focal position by calculation (μm)	Focal depth by calculation (μm)
5900	30.4	5.0	3~5	5.0	3~5	5.0	~4
1725	30.0	2.3	~2	2.0	~1.5	1.8	~2
440	33.5	0.6	~0.5	-	-	0.25	~0.5

4. Conclusion

In conclusions, we have described a fast manner to fabricate micro-nanometric tapered fiber lenses with different geometries on a commercial optical fiber endface. Using this kind of polymer fiber microlens, we have demonstrated the feasibility to image nanostructured sample both using a transmission and a reflection mode. With currently used fiber lenses, a spatial resolution in the order of 100-150 nm has been achieved, which is higher than the resolution by using near field microscopy but lower than the case of the conventional focal microscope. Conversely, using this novel microscopy system, optical characteristics, especially their focal position and focal depths from several hundred nanometers to several microns have been determined.

FDTD calculation results are in good agreement with the experimental measurements, which provides a pondering in-depth for their applications. The exploration of optical properties regarding the fiber tapered micro-nanometric lenses are of great importance for coupling between an optical fiber and optoelectronic devices. Our investigations indicate that such a micro-nanometric fiber lens can serve as a bright nanoscale light source. It will be interesting to exploit potential applications, e.g. imaging of single cells, micro-nanofabrication or optical manipulation using this nanoscale optical field.

Acknowledgments

We thank the National Natural Science Foundation of China (NSFC Grant No. 21107114).

#175636 - $15.00 USD Received 5 Sep 2012; revised 1 Nov 2012; accepted 7 Dec 2012; published 2 Jan 2013